

Available online at www.sciencedirect.com**ScienceDirect**

Procedia Engineering 120 (2015) 578 – 581

**Procedia
Engineering**

www.elsevier.com/locate/procedia

EUROSENSORS 2015

CMOS-compatible Si₃N₄ waveguides for optical biosensing

Paul Mueller^a, Eva Melnik^a, Guenther Koppitsch^b, Jochen Kraft^b, Franz Schrank^b,
Rainer Hainberger^{a*}^a*AIT Austrian Institute of Technology GmbH, 1220 Vienna, Austria*^b*ams AG, 8141 Unterpremstätten, Austria*

Abstract

We present a CMOS-compatible silicon nitride (Si₃N₄) waveguide technology platform suitable for monolithic co-integration with optoelectronics in the visible and <1.1 μm near infrared wavelength region. With an optimized fabrication process employing low-temperature plasma enhanced chemical vapour deposition (PECVD) and reactive ion etching (RIE), propagation losses of 0.86 dB/cm were achieved at λ=850 nm for wire waveguides with a cross section of 600x250 nm². As an example of application we show Mach-Zehnder interferometer based label-free optical detection of the S-protein/S-peptide interaction. Moreover, we present experimental steps towards the realisation of multi-channel biosensors using spiral shaped waveguide structures ensuring a small form factor.

© 2015 Published by Elsevier Ltd. This is an open access article under the CC BY-NC-ND license (<http://creativecommons.org/licenses/by-nc-nd/4.0/>).

Peer-review under responsibility of the organizing committee of EUROSENSORS 2015

Keywords: silicon photonics; silicon nitride; PECVD; optical biosensor

1. Introduction

The ever increasing data volumes to be transmitted over optical fiber links have been the driving force for extensive research and development in the field of silicon-on-insulator (SOI) based photonic integrated circuit technology. A major limitation of the SOI photonic integrated circuit technology platform is the fact that it cannot be used for applications operating at shorter wavelengths in the visible and <1.1 μm near infrared region. However, this spectral region is most relevant for life science and health related applications, which offer a strong potential for photonic integration. Examples are spectroscopy [1], Raman spectroscopy [2], optical coherence tomography [3],

* Corresponding author. Tel.: +43 50550 4304; fax: +43 50550-4399.

E-mail address: rainer.hainberger@ait.ac.at

and biochemical sensing [4,5,6]. In this wavelength region, silicon nitride waveguides offer an attractive alternative for the realisation of PICs. In former optical biosensing demonstrations employing Si_3N_4 waveguides low-pressure chemical vapour deposition (LPCVD) has been used for fabrication. Due to its high temperature LPCVD process it is not compatible with the co-integration of CMOS circuitry. The level of attainable PIC functionality is therefore limited. Moreover, due to strain issues the layer thickness is practically limited to <100-150 nm.

Recently, CMOS compatible silicon nitride waveguides fabricated by low temperature plasma enhanced chemical vapour deposition (PECVD) have attracted increasing interest [7,8,9]. PECVD based silicon nitride waveguides make monolithic integration with silicon photodiodes and electronics possible without the need of wafer or dye bonding. The CMOS-compatible PECVD silicon nitride waveguide fabrication process therefore enables the cost effective implementation of integrated optoelectronics in the <1.1 μm wavelength region. This opens up new market segments including also single use devices e.g. for sensors in the field of medical diagnostics. Moreover, the waveguide layer thickness can be adjusted according to the specific needs of the application without running the risk of strain issues, which gives additional design freedom as compared to LPCVD silicon nitride waveguides.

2. Fabrication

In order to pave the way towards monolithic co-integration with photodiodes and optoelectronic circuitry we developed a waveguide fabrication process employing low-temperature PECVD. The starting material was a blank 200-mm silicon wafer. At a later stage of our development the starting wafer will also include optoelectronic components. First, a silicon dioxide layer with a thickness of 1.5 μm micrometers was deposited by means of PECVD. Next, the silicon nitride waveguide layer with a thickness of 250nm was deposited employing a similar low-temperature PECVD process. Both PECVD process were carried out at temperatures below 400°C. This ensures that the functionality of the integrated optoelectronic components will be maintained. After photolithographic patterning with a minimum feature size of 350nm, the waveguide structures were defined with chemical dry etching. After several cleaning steps, a passivation layer was deposited on top of the waveguide structures. Due to the fact, that silicon nitride does not provide a sufficient etch stop to commonly used etching procedures the photoresist SU8 was used as top passivation. SU8 can be locally removed by means of a standard photolithographic step.

3. Characterisation of the waveguide platform

To enable highly stable and reproducible in and out coupling of the light grating couplers were employed. We determined the insertion losses at a wavelength $\lambda=850$ nm for wire waveguides with a cross section of 600x250 nm², which provide single mode operation necessary for most applications. By measuring the insertion losses of waveguide test structures with different lengths we calculated the propagation loss from the slope (see Fig. 1(a)).

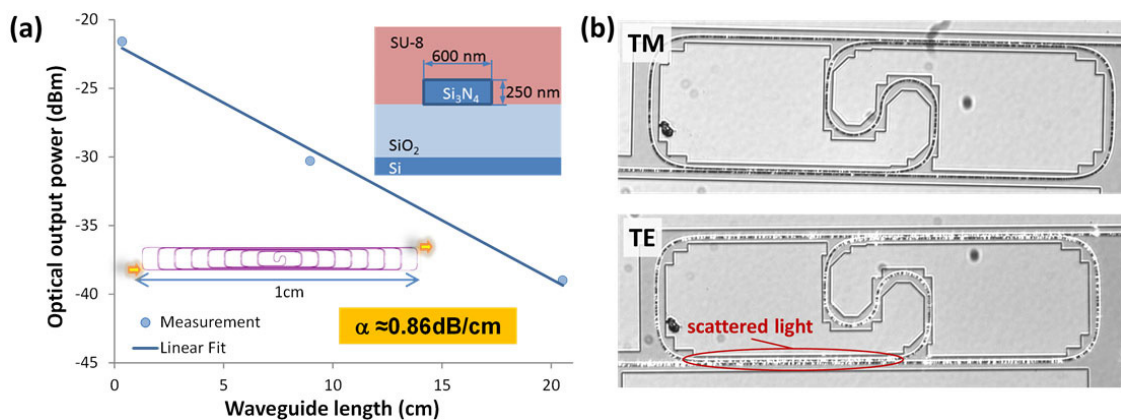


Fig. 1. (a) Measurement of propagation losses for the TM-like mode at $\lambda=850$ nm using PECVD Si_3N_4 waveguides with different lengths; the insets depict the waveguide cross section and the schematic waveguide layout. (b) Micrographs of a waveguide spiral operated with TM (top) and TE polarized light. The bright spots at the waveguides can be attributed to the light which is scattered away from the waveguide.

This revealed a propagation loss of ~ 0.86 dB/cm for the TM-like mode, which is the mode of interest for evanescent wave sensing in wire waveguides. By comparing the losses for the two polarisations, we could identify grain boundaries or small defects in the waveguide material as the main loss source. As shown in the micrographs of Fig. 1(b), the light is scattered away evenly along the entire waveguide. These scattering losses correspond to the different confinement factors of the TM-like compared to the TE-like modes indicating that the losses can be attributed to the waveguide material itself.

4. Optical biosensing as example of application

As an example of application of this waveguide technology platform we implemented integrated optical Mach-Zehnder interferometer (MZI) based biosensors. For waveguide thicknesses of the order of the wavelength a significant part of the optical field extends into the surrounding materials. The binding of biomolecules to the functionalized waveguide surface induces a local refractive index change, which influences this evanescent tail and, consequently, the propagation of the guided light [10] (see Fig. 2(a)). An MZI sensor can be used to exploit this evanescent sensing principle (Fig. 2(b)). In an MZI the light propagating in the input waveguide gets split into two optical paths, the measurement and the reference arm, by means of a Y-junction. The measurement window where the analyte stays in direct contact with the functionalized waveguide surface is approximately 1 cm long. After this interaction length, the light of the measurement arm interferes with the unaltered light of the reference arm in a second Y-branch resulting in a sinusoidal modulation of the optical power. The amount of phase shift of this sinusoidal measurement signal depends on the refractive index change of the biomolecules at the surface cause.

As a first step towards integrated sensor chips, a four channel MZI sensor array was designed (see Fig. 2(c)). Gratings were used for light coupling at a wavelength of ~ 850 nm. After passing the sensor array, the output light was detected by a commercial off-the-shelf CMOS camera, which displayed separate light spots originating from the individual sensor channels. From the brightness of these spots, the MZI modulation of the optical power was deduced. In order to validate the optical sensing performance of the MZI with a 1-cm long measurement arm we chose the S-peptide/S-protein interaction as test model and performed biosensing experiments with different S-protein concentrations (see Fig. 3(a)). The minimum concentration which can be detected was 3 ng/ml.

To further decrease this limit, MZI arms with increased length are beneficial because the sensor response correlates linearly with the waveguide length. Figure 3(b) shows a waveguide spiral with an effective length of 3 cm on a footprint of smaller than 0.2 mm². The comparatively small radius at the spiral center of 50 μ m as well as the spacing between the waveguides of only 4 μ m demonstrate the high degree of integration that is possible with these Si₃N₄ waveguides. We were able to confirm light guiding through these spirals. However, MZI measurements were not possible because a mismatch in propagation losses between reference and measurement arm prevented a suitable

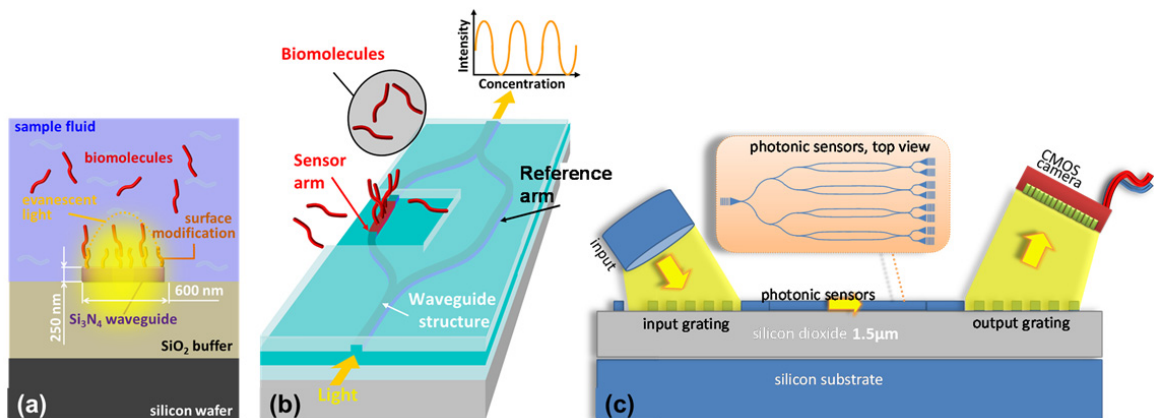


Fig. 2. (a) Cross section of the waveguide illustrating the sensing principle: The evanescent tail of the light propagating in the Si₃N₄ waveguide penetrates the biofunctionalisation layer where the specific binding of target molecules takes place. (b) A Mach-Zehnder interferometer translates the optical phase shift induced by the binding of the biomolecules into a sinusoidal modulation of the output power. (c) Side view (bottom) of the in and out coupling approach. The inset (top) shows the top view on a four channel MZI sensor array.

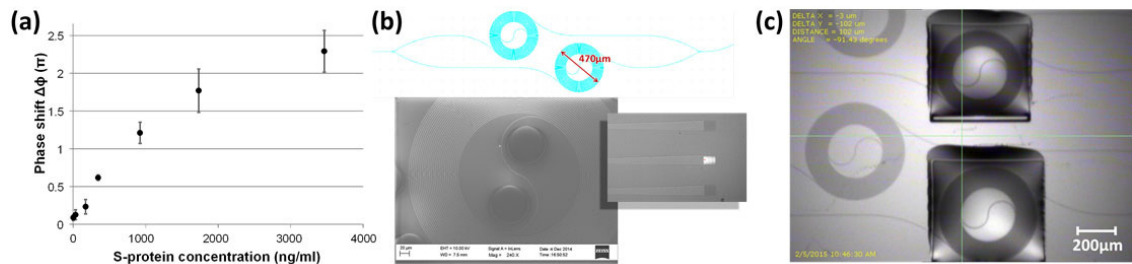


Fig. 3. (a) Measurement of S-peptide/S-protein interaction on an MZI sensor array with four channels as shown in Fig 2(b): Optical phase shift induced by specific binding of S-protein on an MZI biosensor as function of concentration. The Si_3N_4 waveguide surface was silanized, biotinylated, and coated with streptavidin, to which biotinylated S-peptide capture molecules were immobilized. (b) Scanning electron microscope picture (bottom) of a PECVD Si_3N_4 waveguide spiral with 470 μm diameter and 3 cm effective waveguide length to be used as part of an MZI (top); the microscope picture shows the transmitted light deflected by an output grating coupler. (c) Preliminary inkjet printing tests for local deposition of liquids on spiral-shaped Si_3N_4 waveguides within a square-shaped measurement window in the SU-8 cladding.

fringe visibility. This mismatch was caused by the higher propagation loss in the measurement arm, which originates from the stronger confinement of guided light in the silicon nitride waveguide core due to the increased refractive index contrast between the waveguide core and the aqueous cladding as compared to the SU8 cladding.

To overcome this problem, both also the reference arm has to be exposed to the analyte and the measurement arm has to be functionalized locally. By this measure, the optical properties of the two arms will only differ by the biofunctionalisation layer and sensing will become possible. Figure 3(c) shows the result of preliminary inkjet printing tests for local deposition of an aqueous solution, which will enable local biofunctionalisation.

5. Summary

We successfully developed a low-loss silicon nitride waveguide fabrication procedure which is fully compatible with the monolithic co-integration of optoelectronics. The propagation loss of 0.86 dB/cm for the TM-like mode is at the international forefront in this field. The loss can be mainly attributed to the waveguide material, where room for optimisation of the fabrication process is still given. This waveguide technology platform was employed for a 4-channel MZI biosensor array and a strategy was devised how the sensor response can be further increased by means of locally functionalized spiral shaped waveguide MZIs.

References

- [1] D. Martens, A.Z. Subramanian, S. Pathak, M. Vanslambrouck, P. Bienstman, W. Bogaerts, R.G. Baets, Compact Silicon Nitride Arrayed Waveguide Gratings for Very Near-Infrared Wavelengths, *IEEE Photon. Technol. Lett.* 27 (2015) 137–140.
- [2] A. Dhakal, A.Z. Subramanian, P. Wuytens, F. Peyskens, N. Le Thomas, R. Baets, Evanescent excitation and collection of spontaneous Raman spectra using silicon nitride nanophotonic waveguides, *Optics Letters* 39(13), pp. 4025–4028 (2014)
- [3] G. Yurtsever, B. Považay, A. Alex, B. Zabihian, W. Drexler, R. Baets, Photonic integrated Mach-Zehnder interferometer with an on-chip reference arm for optical coherence tomography, *Biomed. Opt. Express* 5 (2014) 1050-1061.
- [4] A. Ymeti, J. Greve, P.V. Lambeck, T. Wink, van Hövell, Stephan W.F.M., T.A.M. Beumer, R.R. Wijn, R.G. Heideman, V. Subramaniam, J.S. Kanger, Fast, ultrasensitive virus detection using a Young interferometer sensor, *Nano Letters* 7 (2007) 394–397.
- [5] F. Ghasemi, A.A. Eftekhar, D.S. Gottfried, X. Song, R.D. Cummings, A. Adibi, A.N. Cartwright, D.V. Nicolau, Self-referenced silicon nitride array microring biosensor for toxin detection using glycans at visible wavelength, *Proc of the SPIE Vol. 8594* (2013) 85940A.
- [6] Q. Liu, X. Tu, K.Woo Kim, J.Sheng Kee, Y. Shin, K. Han, Y.-J. Yoon, G.-Q. Lo, M.K. Park, Highly sensitive Mach-Zehnder interferometer biosensor based on silicon nitride slot waveguide, *Sensors and Actuators B: Chemical* 188 (2013) 681–688.
- [7] S. Romero-Garcia, F. Merget, F. Zhong, H. Finkelstein, J. Witzens, Silicon nitride CMOS-compatible platform for integrated photonics applications at visible wavelengths, *Opt. Express* 21 (2013) 14036–14046.
- [8] A.Z. Subramanian, P. Neutens, A. Dhakal, R. Jansen, T. Claes, X. Rottenberg, F. Peyskens, S. Selvaraja, P. Helin, B. DuBois, K. Leyssens, S. Severi, P. Deshpande, Low-Loss Single mode PECVD Silicon Nitride Photonic Wire Waveguides for 532–900 nm Wavelength Window Fabricated Within a CMOS Pilot Line, *IEEE Photonics J.* 5 (2013) 2202809.
- [9] P. Neutens et al. Development of a CMOS Compatible Biophotonics Platform Based on SiN Nanophotonic Waveguides, *CLEO 2014*, JTh2A.31.
- [10] K. Tiefenthaler, W. Lukoz, Sensitivity of grating couplers as integrated-optical chemical sensors, *J. Opt. Soc. Am. B* 6 (1989) 209–220.